Modelling the stratospheric budget of beryllium isotopes

Gilles Delaygue, Slimane Bekki, Edouard Bard

Tellus SERIES B CHEMICAL AND PHYSICAL METEOROLOGY
PUBLISHED BY THE INTERNATIONAL METEOROLOGICAL INSTITUTE IN STOCKHOLM

Modelling the stratospheric budget of beryllium isotopes

By GILLES DELAYGUE[1]*, SLIMANE BEKKI[2] and EDOUARD BARD[3], [1]*Laboratoire de glaciologie et géophysique de l'environnement, University Grenoble-Alpes, FR-38041 Grenoble, France;* [2]*UPMC, UVSQ, CNRS/INSU, LATMOS-IPSL, FR-78280 Guyancourt, France;* [3]*CEREGE, Aix Marseille University, CNRS, IRD, Collège de France, FR-13545 Aix-en-Provence, France*

(Manuscript received 19 May 2015; in final form 29 July 2015)

ABSTRACT

A global 2-D (latitude–altitude) model describing both the stratospheric circulation and the detailed formation and growth of stratospheric aerosols is used to simulate the stratospheric cycle of cosmogenic isotopes of beryllium, Be-7 and Be-10. These isotopes have been extensively used as tracers of stratospheric air, as well as of solar variability. The simulation of these isotopes is used to quantify the relative importance of transport, microphysic processes related to aerosols, and radioactive decay, on their concentrations. Calculations of model budget show that the vertical transfer of these isotopes due to the aerosol sedimentation contributes to about half of the stratospheric Be-10 flux into the troposphere, but is negligible for the Be-7 budget. The simulated residence time of these isotopes in the lower stratosphere is monotonically related to the age of air; however, this relationship is neither linear nor uniform, which biases the age of air inferred from these isotopes.

Keywords: stratospheric dynamics, aerosols and particles, geochemical cycles, cosmic rays

1. Introduction

Beryllium-10 (Be-10) and beryllium-7 (Be-7) are the radioactive isotopes of beryllium, with very contrasted half-lives: about 1.4 million years for Be-10 and only 53 d for Be-7. Both are cosmogenic isotopes, produced in the atmosphere as a result of spallation of atmospheric gases nuclei (mostly oxygen and nitrogen) by secondary neutrons and protons formed by galactic cosmic rays (GCR) through a cascade of nuclear reactions. From the stratosphere to the troposphere, the flux of secondary nucleons decreases and the density of targets (oxygen and nitrogen) increases: this results in beryllium production rates that are approximately twice as high in the stratosphere as in the troposphere (e.g. Lal and Peters, 1962). Once produced, these elements quickly attach to and are entrained by aerosols.

Aerosols are transported by the winds and also redistributed vertically by gravitational sedimentation. They are ultimately removed from the atmosphere by wet and dry deposition in the troposphere. Because of the efficient removal by wet deposition (i.e. precipitation), aerosols have a mean residence time of less than a week in the troposphere, whereas the residence time is about a couple of years typically in the stratosphere. As a result, beryllium concentrations in the troposphere are one to two orders of magnitude lower than in the stratosphere (e.g. Bhandari et al., 1966; McHargue and Damon, 1991). This makes beryllium concentrations a potential tracer of stratospheric air inputs into the troposphere.

In the 1950s and 1960s, Be-7, along with other radioactive isotopes attached to aerosols, has been measured up to the stratosphere in order to constrain the stratospheric circulation and the troposphere–stratosphere exchanges (STE) (e.g. Bhandari et al., 1966). A special concern at that time was about fallouts of radioactive debris from nuclear bomb tests. A key information on the timescale of stratospheric transport and mixing of aerosols is how close a measured concentration of a radioactive isotope is to the equilibrium concentration calculated by assuming that production and radioactive decay are perfectly balanced. Depending on the scientific field, this concentration has been called 'secular equilibrium', 'saturation' or simply 'chemical steady-state' concentration. When measured Be-7 concentrations significantly deviate from secular equilibrium values, it implies that other processes (notably advection, mixing or gravitational sedimentation in the stratosphere, and wet and dry deposition in the troposphere) operate on timescales similar or shorter than the radioactive decay timescale. Therefore, the extent of deviation from saturation contains some information on atmospheric transport pathways and timescales.

*Corresponding author.
email: gilles.delaygue@ujf-grenoble.fr

Citation: Tellus B 2015, **67**, 28582, http://dx.doi.org/10.3402/tellusb.v67.28582

Concentrations of Be-7 measured in the lower stratosphere have been found to be distinctively lower than saturation values ('undersaturation') at high latitudes, suggesting that the transport of aerosols out of this region is a significant sink compared to the $\sim$2.5 month decay period of Be-7. Further, Bhandari et al. (1966) attempted to estimate the contribution of sedimentation ('gravitational settling') to the removal of aerosols (and thus of cosmogenic atoms). In the polar lower stratosphere, they estimated a (partial) characteristic timescale for removal by sedimentation of about 3 yr, compared to a characteristic timescale for overall removal of ca. 10 months.

The use of cosmogenic isotopes as air tracers has been refined by combining isotopes and considering ratios of isotopes concentrations, for instance Be-7/P-32 and Na-22/Be-7. Using ratios of isotopes concentrations instead of concentrations themselves has several advantages. A technical advantage is that the uncertainties related to the volume of air pumped to collect aerosols affect concentration measurements of individual isotopes but not the concentrations ratio. In addition, isotopes concentrations ratios are much more sensitive to the difference between the radioactive decay rates of isotopes and thus to the time elapsed since the formation of the isotopes, than to transport processes such as advection of air masses or sedimentation of aerosols, which affect about equally both concentrations of cosmogenic isotopes. In a sense, concentrations ratios can also be viewed as potential indicators of the age of air since the formation of the isotopes. Raisbeck et al. (1981) proposed to consider the Be-10/Be-7 ratio of aerosols as a new tracer of stratospheric air. Indeed, the ratio of Be-10 and Be-7 production rates is rather homogeneous in the stratosphere, and both isotopes have similar removal rates but very contrasted radioactivities. In an air mass with no other source of beryllium than production, Be-10 would accumulate and the Be-10/Be-7 ratio would increase over time, with the removal of aerosols limiting this increase. Although measurements of Be-10 were technically very difficult, and thus very limited in the stratosphere (e.g. Jordan et al., 2003), the available measurements have showed that Be-10 and Be-7 concentrations and their ratio are very different in the troposphere and in the stratosphere, and that their ratio could be used successfully as a tracer of stratospheric inputs to the troposphere (e.g. Dibb et al., 1994).

In order to interpret measurements of beryllium concentrations, beryllium isotopes have been implemented in models of atmospheric circulation. A lot of attention has been paid to resolve and simulate correctly the complex tropospheric processes driving the aerosols and hence beryllium isotope cycle within the troposphere, notably deposition processes, and their spatio-temporal variability. These model developments partly originated from the need to understand and reproduce the strong variability seen in the measurements of beryllium isotopes concentration. The first modelling studies were focused on the stratosphere–troposphere exchange of air and on the scavenging efficiency of air tracers in the troposphere to quantify the vertical mixing (e.g. Brost et al., 1991; Rehfeld and Heimann, 1995; Koch et al., 1996; Koch and Rind, 1998; Land and Feichter, 2003). Later on, the focus moved onto simulating the impact of solar variability on the Be-10 production, atmospheric concentration and deposition, in order to help the interpretation of Be-10 records (e.g. Field et al., 2006; Heikkilä et al., 2008b).

A key question tackled in several of these studies was where and how much stratospheric air enters the troposphere and gets mixed with tropospheric air, and evidence of strong stratosphere–troposphere exchanges has been found at mid-latitudes (e.g. Stohl et al., 2003). Cosmogenic isotopes can help deciphering these regions of STE with stronger fluxes coming from the stratosphere. Fallouts of bomb-produced Sr-90 measured in the 1950s and 1960s were used to already infer that STE are concentrated at mid-latitudes (e.g. Junge, 1963). Lal and Peters (1967, Fig. 22) further estimated that the stratospheric contribution to the total deposition flux of long-lived cosmogenic isotopes should peak at $\sim$75% at mid-latitudes, and decrease to $\sim$25% at low latitudes. Using a full general circulation model (GCM), Heikkilä et al. (2009) found a similar peak for the stratospheric contribution to the Be-10 flux at mid-latitudes (75%), but rather high stratospheric contributions elsewhere (at least 50%), implying that the stratospheric Be-10 flux did not vary as much regionally, at least in this model.

How well a model performs with respect to the latitudinal distribution of the Be-10 deposition depends on how well the model simulates not only STEs and tropospheric aerosol processes but also stratospheric processes controlling Be-10 concentrations and latitudinal gradients in the lowermost stratosphere (next to the tropopause region). This requires a rather realistic description of the stratosphere and of microphysical processes controlling stratospheric aerosols because, as already pointed out, the stratospheric Be cycle is intimately linked to the stratospheric cycle of aerosol particles. Indeed, once produced in the stratosphere, beryllium atoms stick to aerosols whose sedimentation affects the distribution of beryllium in the stratosphere. Stratospheric aerosols are essentially composed of sulphuric acid and water and the main non-volcanic source of sulphur to the stratosphere is surface emissions of carbonyl sulphide (OCS), the only longed-lived sulphur species (Crutzen, 1976; Turco et al., 1982; SPARC, 2006, and references therein). So far, atmospheric modelling of beryllium isotopes has been mostly focused on the tropospheric cycle with a great deal of model developments being put into detailed

representations of beryllium tropospheric processes (such as wet versus dry deposition of aerosols and so on). In contrast, treatments of stratospheric processes relevant for beryllium have been simplified. For instance, the important stratospheric process for the global beryllium distribution is the aerosol gravitational sedimentation that drives the vertical redistribution and residence time of beryllium in the stratosphere. Nonetheless, the effect of aerosol sedimentation in the stratosphere is poorly parameterised in global beryllium isotopes models. The two models of reference for the beryllium are the ECHAM (Heikkilä et al., 2008a, 2008b) and the GISS (Koch and Rind, 1998; Field et al., 2006; Koch et al., 2006) GCMs. In the GISS model, stratospheric aerosol particles are assumed to be particles with a constant radius of 0.1 μm, typical of the mean radius of background (i.e. non-volcanic) aerosols, that sediment throughout the entire stratosphere. However, all the measurements and model calculations show that the size of background aerosol particles varies widely with altitude and latitude within the stratosphere (Turco et al., 1982; SPARC, 2006, and references therein). As the aerosol sedimentation velocity varies very strongly with the size of the aerosol (Seinfeld and Pandis, 2006), aerosol sedimentation rate also varies widely within the stratosphere. In addition, as stratospheric aerosols evaporate above 30–35 km because of the temperature increase with altitude, there is no sedimentation in the middle and upper stratosphere. This is not the case in the GISS model (Field et al., 2006). In the ECHAM model, the effect of aerosol sedimentation on beryllium isotopes is calculated throughout the atmospheric column based on the aerosol distribution and size calculated on-line by the HAM aerosol module (Stier et al., 2005). However, stratospheric aerosol particle loading is way too small in the ECHAM-HAM model because OCS, the main background (non-volcanic) source of sulphur to the stratosphere, is not included in the model (Stier et al., 2005). In addition, the top of the older versions of the ECHAM-HAM model was at 10 mb (about 31 km) (Heikkilä et al., 2008a, 2008b), preventing it from simulating correctly the timescale and pathways of the stratospheric general circulation (Bunzel and Schmidt, 2013). Although these global 3-D models have shown remarkable skills in simulating the tropospheric beryllium cycle (e.g. Usoskin et al., 2009), they do not include yet adequate descriptions of stratospheric aerosol microphysical processes for the study of the stratospheric beryllium cycle. We note that the SOCOL 3-D chemistry–climate model has been very recently coupled to the detailed aerosol microphysics of the 2-D AER model (Sheng et al., 2015). When equipped with the beryllium isotopes, this model will be of great help to study regional features of the stratospheric beryllium cycle.

Two aspects of the stratospheric aerosols are of importance for the beryllium cycle. First, the growth of aerosols during their general transport from the tropics to mid- and high latitudes is fundamental in controlling the global distribution of aerosol sedimentation rate and hence Be-10 and Be-7 concentrations. Second, because of the process of sedimentation, beryllium atoms are not simple tracers of stratospheric air motions. As a result, the estimations of stratospheric 'age of air' from Be-10 and Be-7 concentrations, based on the residence time of aerosols in an isolated air mass (e.g. Raisbeck et al., 1981; Dibb et al., 1994) may be somehow biased, especially compared to estimates based on chemical tracers such as SF_6 or CO_2 that are not affected by sedimentation. The removal of aerosols by sedimentation should bias the residence time of aerosols and the inferred 'age of air' to lower values.

The focus of the present work is the global beryllium stratospheric cycle that has not been investigated realistically since the 1960s. We use a 2-D stratospheric circulation model which benefits from a detailed description of stratospheric aerosol life cycle (Section 2). Despite its very coarse resolution, this model is able to reproduce the large scale features of both the stratospheric circulation and aerosols distribution. Beryllium isotopes are introduced as tracers in this model (Section 3), in order to analyse their distribution and budget (Section 4). In particular, we study the importance of the general stratospheric circulation, aerosol sedimentation and radioactive decay, in determining the beryllium isotopes concentrations and their distribution in the stratosphere (Sections 5 and 6). We also study the impact of the aerosol sedimentation on the residence time of beryllium isotopes, and the bias on the inferred 'age of air' (Section 7).

2. Description of the stratospheric model

2.1. Dynamics

The Cambridge 2-D model is a well-established global 2-D (latitude–altitude) fully interactive radiative chemical transport model for the stratosphere (Harwood and Pyle, 1980). 2-D models are well suited for global stratospheric studies because circulation and global distribution of tracers tend to be zonal in the stratosphere (Brasseur and Solomon, 2005, and references therein). For instance, they are the reference tools for the calculations of ozone depletion potential, global warming potential and individual contributions of CH_4, N_2O and CO_2 to the evolution of stratospheric ozone, within the framework of WMO/UNEP model assessment of stratospheric ozone (WMO, 2011, 2014).

Our 2-D model extends from pole to pole and from the surface to around 95 km with a resolution of 3.5 km vertically and 9.5° horizontally (Fig. 1). Two-dimensional forms of the thermodynamic, momentum and tracer continuity equations are solved for each time step of 4 hours to

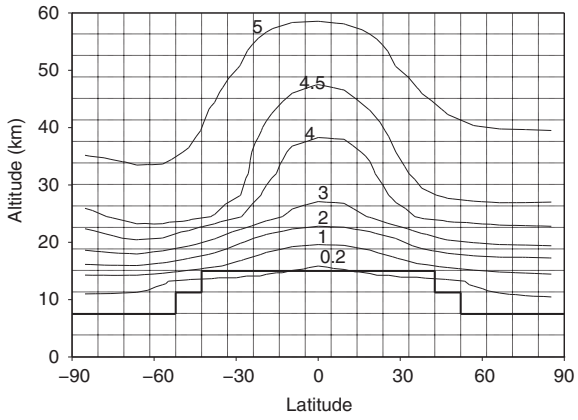

Fig. 1. Simulated time spent by an air mass in the stratosphere, in years ('age of stratospheric air'). The thin dashed line is the model grid; the thick line is the model tropopause. Note that the crossing of the tropopause by the 0.2 yr isoline is due to interpolating on the too coarse grid.

give updated fields of temperature, velocity and chemical species. The mean circulation is calculated from forcing terms that include latent and radiative heating and eddy transport processes. This allows the model, in principle, to include a description of radiative and chemical feedbacks. The transport in the model is split into two parts: advection due to the zonal mean circulation, and transport arising from departures from the zonal mean, the eddies. The eddy diffusion coefficients are specified based on observed tracer global distributions (Law and Pyle, 1993). Note that the model tropopause is defined by constant pressure levels that depend on the latitude, so that its elevation ranges from roughly 7 km in polar regions to 15 km in the tropics (Fig. 1). The net heating rates are specified in the troposphere, from -1.5 K/day in the lower troposphere to -0.75 K/day in the upper troposphere. These rates are added to latent and sensible heat fluxes that are also specified. These fluxes vary sinusoidally through the year at each latitude. In contrast, the stratospheric radiation scheme in the model is complex, including the detailed treatment of both longwave and shortwave components. The model has a simple interactive water vapour scheme in the troposphere. Briefly, water vapour is transported and removed as precipitation if the vapour pressure in a particular grid box exceeds 80% of the saturation pressure. Air at the surface is assumed to be saturated in H_2O (with respect to the sea surface temperature). The resolution in the model troposphere is fairly coarse and the model does not contain a proper treatment of the boundary layer. Nonetheless, the model captures most basic dynamical features found in the troposphere: a Hadley circulation in the tropics, a Ferrell cell in mid-latitudes, and an indirect polar cell at high latitudes (Law and Pyle, 1993). However, given these limitations, the 2-D model is best thought of as a model of the upper troposphere and of the stratosphere. An obvious advantage of such coarse resolution is that simulations can be run quickly with a standard computer, and this allows sensitivity experiments to be conducted.

2.2. *Chemistry and aerosol microphysics*

The chemistry scheme accounts for Ox, HOx, NOy, Cly, Bry and CHOx chemistry. The treatment of chemical species in the model is simplified by using the family approach. Photochemical steady state is assumed for the species with short chemical lifetimes compared to their dynamical lifetimes, that is, distributions governed by chemistry rather than transport. Then, it is only necessary to transport the family as a whole, allowing large savings in computer time.

Reaction rates which depend on temperature and pressure are computed each time step except for the photolysis rates, which are calculated every 10 d. In general, the photochemical data are taken from Sander et al. (2011) recommendations.

The sulphur chemistry is based on Bekki and Pyle (1992) and Bekki (1995). Stratospheric aerosol particles are treated as liquid droplets of sulphuric acid solution. Sulphuric particles are produced by binary homogeneous nucleation and grow by coagulation and co-condensation of H_2SO_4 and water. Their formation and evolution are explicitly simulated using a sectional aerosol scheme. Stratospheric aerosol schemes differ from tropospheric aerosol models in that resolving the size distribution of aerosol particles is crucial to predicting the correct sedimentation rate and therefore the lifetime and global distribution of stratospheric particles. In the troposphere, only particles larger than ~ 1 μm settle appreciably, whereas the thinner air in the stratosphere causes sedimentation rates to be a strong function of both particle radius and air density. Even particles of 0.01 μm have significant sedimentation rates at 30 km (e.g. SPARC, 2006, Fig. 6.5). Tropospheric aerosol models typically deal only with total aerosol mass, but may assume a lognormal distribution to resolve the particle sizes. Like all stratospheric models, our model resolves aerosol sizes into sections, or 'bins' (using a geometrical factor between the volumes of consecutive bins), with each bin size transported separately. These types of aerosol schemes are usually referred to as 'fully size-resolving' aerosol schemes. Since the computational cost of resolving an additional dimension (i.e. size space) is very high, size-resolving schemes were only used in two-dimensional models and low-resolution global three-dimensional models (SPARC, 2006). In our model, the aerosol size distribution covers a range of radii from 0.01 to 2.5 μm and is divided into 25 bins. Microphysical processes (nucleation, condensation/evaporation, coagulation, sedimentation) determine the evolution of the aerosol

concentration in each size bin. Aerosol particles are predominantly removed from the model stratosphere by gravitational sedimentation, followed by wet and dry depositions in the troposphere, with wet deposition being the overwhelming removal process. The scavenging processes are parameterised in a simple way in the 2-D model; wet deposition is modelled as the reciprocal of a lifetime (with respect to rainout and washout) following Logan et al. (1981) with the scavenging rates varying with altitude (Fig. 2). These scavenging rates have been adjusted in order to correctly reproduce tropospheric concentrations of soluble species.

The variations of the stratospheric source gas mixing ratios (CO_2, CH_4, N_2O, CFCs...) at the surface during the integrations are based on a recommended WMO scenario (WMO, 2011). Surface mixing ratios of sulphur source gases, carbonyl sulphide OCS and dimethyl sulphide (DMS), are kept constant at 500 pptv; the high DMS surface mixing ratio ensures realistic concentrations of SO_2 in the model's middle and upper troposphere. OCS is the only long-lived sulphur species and hence the dominant stratospheric source of sulphur during background (non-volcanic) period.

The overall performances of the model regarding stratospheric aerosols have been extensively evaluated against other stratospheric aerosol models and a range of observations within the framework of international model intercomparison and validation program (e.g. SPARC, 2006). Our model simulations of the stratospheric aerosol cycle, aerosol distribution and their perturbation by the Mount Pinatubo volcanic eruption have been found to compare extremely well with other model simulations and observations (Bekki and Pyle, 1994; SPARC, 2006).

2.3. *Diagnostic of the model dynamics: age of stratospheric air*

As a diagnostic of the simulated transport of stratospheric air, an 'age of air' tracer has been included in the model following the Waugh and Hall (2002) approach [their eq. (10)].

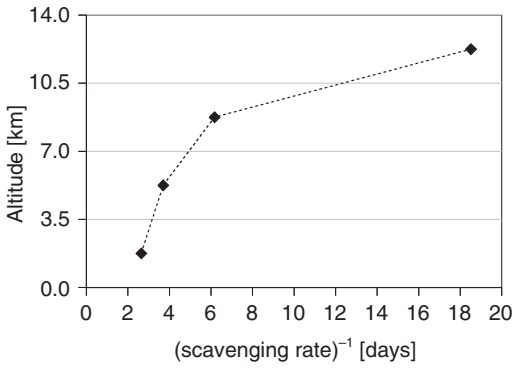

Fig. 2. Scavenging rates applied to particles and beryllium atoms in the model troposphere.

The tropical tropopause is thought to be the entrance point of tropospheric air into the stratosphere. Therefore, the value of the tracer at the tropical tropopause is simply incremented like a timer. The tracer is transported through the atmosphere and the difference between the tropical tropopause value and the tracer values at a given grid box provides the mean age of air at this grid box, that is, the time that has elapsed since the air has entered the stratosphere. This age should correspond to the mean residence time of stratospheric air.

Figure 1 shows the simulated global age of air distribution. The values compare well with estimates of 2-D and 3-D stratospheric models (Hall et al., 1999), but are consistently too young compared to the 'mean age of air' inferred from measurements of long-lived chemical species (Waugh and Hall, 2002; Haenel et al., 2015). The simulated ages are too young by $\sim$1 yr at high latitudes, which is a deficiency common to global 2-D models because they have difficulties reproducing correctly the stratospheric diabatic descent in polar regions during winter (Chipperfield and Pyle, 1988). Also, the horizontal gradient around the tropics, defining the so-called 'tropical pipe', is too weak in the model, which is too much diffusive in this respect.

2.4. *Introduction of beryllium isotopes in the model*

Two tracers of Be-10 and Be-7 have been added to the model. Once produced, Be-10 and Be-7 atoms are supposed to stick to particles that are present and are then transported like any other tracer. In addition, they are also subject to sedimentation and scavenging along with the particles. Sedimentation of particles strongly depends on their size: this is why the model ability to account for the spatio-temporal changes in stratospheric size distribution is important. As discussed in the Introduction, 3-D models used for beryllium studies and equipped with microphysics of aerosols do also simulate sedimentation of particles, but with less detail in its treatment in the stratosphere. In our model, sedimentation rates are calculated for each of the 25 modes of particles, and then applied to beryllium atoms by assuming that they are homogeneously distributed in the particles. This latter simplification should not have a large influence on sedimentation rates of beryllium atoms because actual particle population and sedimentation are dominated by large particles.

In the model troposphere, beryllium atoms are scavenged along with the aerosol particles. The highly simplified scavenging scheme (see above) prevents us to simulate realistically deposition fluxes and tropospheric concentrations measured at specific sites. For this reason, the main focus of the present study is the stratospheric cycle of beryllium.

3. Production of cosmogenic beryllium atoms

Production of beryllium atoms by spallation of oxygen and nitrogen atoms follows a complex pathway. Basically, ionised particles composing the GCR are deviated by the heliospheric magnetic field and the solar wind. This is accounted for by the deceleration parameter Φ called the solar modulation parameter (Gleeson and Axford, 1968). We choose a constant value $\Phi = 600$ MV which corresponds approximately to the average value over the last solar cycles (Usoskin et al., 2011). GCR are later deviated by the geomagnetic field, which roughly resembles a slightly tilted dipole. This deviation is accounted for by the magnetic cutoff rigidity, that is, the minimal energy of particles required to penetrate the atmosphere at a given location. We use here the vertical effective cutoff rigidity (Rc) estimated for the year 1950 by Smart and Shea (2003), as given by Lifton et al. (2008). We use Rc estimates for year 1950 rather than for a more recent one because this is a reference year in several studies. Changes in the geomagnetic field and poles locations have been limited since 1950 and this has little impact on our results. In theory, cutoff rigidity should be calculated at each atmospheric level. However, we use instead the vertical effective rigidity for two reasons. Firstly, rigidity varies inversely to the squared distance to the magnetic dipole, so that the change across the model atmosphere is less than 4%. Secondly, this parameter has been used by Usoskin and Kovaltsov (2008) and Kovaltsov and Usoskin (2010) to calculate the beryllium isotopes production rates which are used here, so that we use Rc for consistency.

GCR interact with nuclei in the atmosphere, producing both cosmogenic nuclei and secondary nucleons which further interact with nuclei. This cascade of interactions has been calculated in several studies. We use recent ones, Usoskin and Kovaltsov (2008) for Be-7 production and Kovaltsov and Usoskin (2010) for Be-10 production. These studies have brought several improvements, especially recent cross section estimates for the targets O and N, and curved geometry of the atmosphere to better simulate interactions in the stratosphere. The most important point here is that both studies use the same spectrum of energies for GCR and the same numerical models for simulating interactions at the origin of Be-10 and Be-7 production. Such consistency is fundamental for our study, since any linear bias common to both Be-10 and Be-7 production rates vanishes in their ratio.

Both studies have provided sets of tabulated production rates for different solar modulation and cutoff rigidity values. We have combined these tabulated production rates with the 3-D cutoff rigidity field provided by Lifton et al. (2008) in order to calculate 3-D fields of Be-10 and Be-7 production rates for $\Phi = 600$ MV. These rates were then zonally averaged to fit our 2-D model grid. Note that the tilt of the geomagnetic poles clearly translates into both 3-D and 2-D production rates; this is why our 2-D fields are not exactly symmetric between both hemispheres (Fig. 3).

We find a global Be-10 production rate of $P_{10} \sim 1.5 \times 10^{17}$ atoms/s and a global Be-7 production rate of $P_7 \sim 3.3 \times 10^{17}$ atoms/s, which correspond to potential globally averaged deposition fluxes of ca. 0.029 atoms/s/cm^2 and 0.065 atoms/s/cm^2, respectively. These values are in good agreement with the rate of 0.032 Be-10 atoms/s/cm^2 found by Kovaltsov and Usoskin (2010) for a slightly lower Φ value of 550 MV, and of 0.062 Be-7 atoms/s/cm^2 found by Usoskin and Kovaltsov (2008) for a higher Φ value of 700 MV. These production rates are about 50% higher than those calculated by Masarik and Beer (2009). It is far beyond the scope of this work to discuss the uncertainty on these production rates, and we refer to the discussions by Usoskin and Kovaltsov (2008) and Kovaltsov and Usoskin (2010). Again, the most important point for this work is that Be-10 and Be-7 production rates have been calculated consistently.

Concentrations of species in the atmosphere, and similarly production rates, can be expressed in different ways: as absolute concentrations, mixing ratios (when normalised to

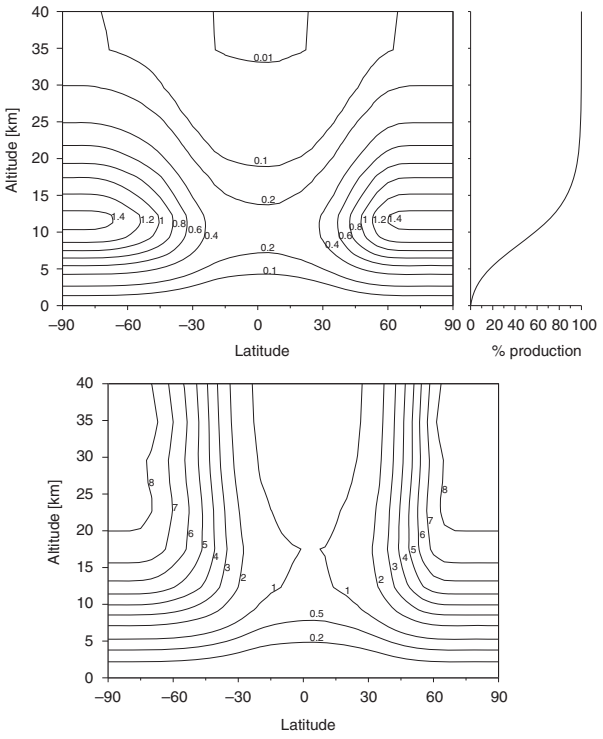

Fig. 3. Production rate of Be-10 for $\Phi = 600$ MV. Altitudes are approximate. Top: production rate independent of air expressed in atoms per year per actual cubic centimetre. Cumulated profile on the right. Bottom: production rate dependent of air, expressed in atoms per year per standard cubic centimetre.

air density), or normalised to standard conditions of temperature and pressure (STP), in order to account for density changes due to temperature and pressure during transport. Be-10 and Be-7 are not conserved quantities with respect to air molecules because (1) as cosmogenic species, they are produced in situ and not injected with air into the stratosphere, (2) they are removed from air masses by sedimentation of aerosols, and (3) decay of Be-7 is important during its transport in the stratosphere. For these reasons, global distribution of production rates is displayed on Fig. 3 with two different units, absolute terms and normalised to STP conditions. The spatial variations in production rate arise from the interplay between the cutoff rigidity, which controls the penetration of GCRs, and the density of atmosphere, which controls both the probability of spallation and the intensity of the neutron cascade. These distributions are actually very close to the ones calculated by Lal and Peters (1967, Fig. 20) and McHargue and Damon (1991, Fig. 1). In absolute terms, the maximum rates, slightly above 1.4 atoms/yr/cm^3, are found at high latitudes around 11 km. The minimum rates are located in the tropics, both at the surface and at high altitudes. When normalised to STP, production rates increase with latitude; they also increase with altitude up to 15–20 km, above which they are virtually constant at a given latitude.

An interesting view of this production is vertically integrated, since this would correspond to the surface deposition of Be-10 if no horizontal transport existed. As stratosphere and troposphere have significantly different transport timescales and are largely decoupled, the vertical integration is more insightful when applied separately to each of these reservoirs. However, the vertically integrated productions are quite sensitive to the definition of these reservoirs (i.e. of the tropopause), as shown by Fig. 4. As expected from Fig. 3, the stratospheric vertically integrated production is maximum at high latitudes, stronger by an order of magnitude than the production at low latitudes. For the troposphere, the picture is somehow different since its thickness decreases with latitude. In our model this decrease almost compensates the stronger production at high latitudes (Fig. 4 top). Of course this is not the case when integrating over atmospheric layers of constant thickness (Fig. 4 bottom). Globally, when using the tropopause definition of our model, we find that about 62% of the total production takes place in the stratosphere and 38% in the troposphere.

The production rates of Be-10 are on average three times lower than the Be-7 rates, but the Be-10/Be-7 production ratio is not homogeneous. As shown by Fig. 5, this ratio decreases with altitude, ranging from maxima of 0.8 at the polar surface to minima of around 0.32 between 25 and 30 km. Above ca. 35 km, the ratio is close to 0.35. This ratio distribution is close to the one estimated by Masarik and Beer (1999), as published by Heikkilä et al. (2008a), but the values are lower especially at high elevations: for instance the 0.4 value is found at about 15 km with the production rates we use compared to $\sim$26 km (depth of 30 g/cm^2) with the Masarik and Beer data. Interestingly, this production ratio is hardly sensitive to solar activity: changing the modulation parameter Φ from 600 MV to 1000 MV affects the production ratio by less than 2%. Previous studies

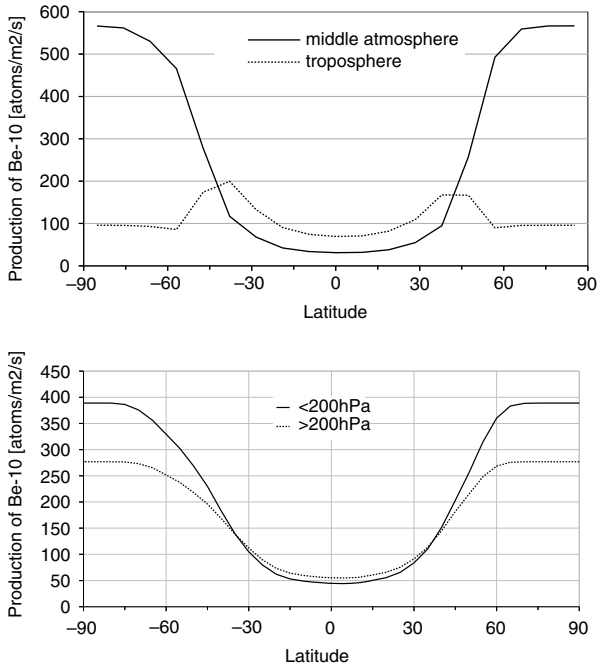

Fig. 4. Vertically integrated production rate of Be-10 through the middle and lower parts of the atmosphere to sea level. (Top) Vertical definition based on our model definition of the tropopause, and (bottom) definition based on pressure.

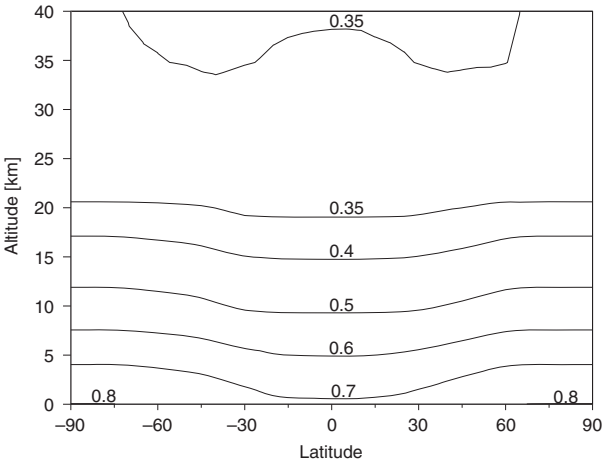

Fig. 5. Ratio of Be-10 to Be-7 production rates.

(e.g. Raisbeck et al., 1981; Jordan et al., 2003) considered the production ratio as homogeneous and used an average value of 0.5–0.6 to infer a mean age of air from measurements of the Be-10/Be-7 ratio. With the production data we use here, such values are typically found in the upper troposphere and tropopause regions, but the production ratio drops to 0.4 and even 0.35 just above the tropopause, at an altitude of approximately 20 km. We will discuss in the following the consequence of using a mean value of 0.5 on the inferred mean age of air.

4. Simulated beryllium concentrations

These production rates of Be-10 and Be-7 are prescribed in our 2-D atmospheric model. The model is run for 100 yr with constant forcings (i.e. surface mixing ratios of stratospheric source gases) to ensure that there is no trend in the dynamics and chemistry of the model atmosphere. Then, the last 20 yr of the run are analysed by calculating averaged quantities such as mean annual cycles.

There are many more measurements of Be-7 than of Be-10, and thus we first focus on the simulated distribution of Be-7 shown by Fig. 6. Model-calculated concentrations are normalised to STP in order to compare them to measurements. It is worth keeping in mind that such a concentration unit does not provide a correct view of the actual distribution, in absolute terms.

There are a number of factors that make such comparisons with measurements difficult:

(1) The very coarse resolution of the model makes it difficult to compare spotty data to large scale average values from the model, especially close to the tropopause where large gradients do exist.
(2) The necessity to restrict comparison to stratospheric measurements; stratospheric concentrations are much more uniform and much less variable than tropospheric concentrations. Simulated tropospheric concentrations are not meant to be very realistic because of the very simplified removal scheme in the troposphere.
(3) Measurements were done at different times of the year: Fig. 6 shows the most contrasted concentrations in order to provide a seasonal range to compare with measurements.
(4) The varying solar activity affects both the beryllium production and the stratospheric meridional circulation (e.g. Kodera and Kuroda, 2002). During a solar cycle, variations of the beryllium production are very limited at low latitudes. However, they are very significant at mid to high latitudes, approximately $\pm 20\%$ around the mean values calculated for an average solar modulation factor $\Phi = 600$ MV (e.g. Fig. 3 of Masarik and Beer, 2009). Hence, solar-driven variations of at least 20% in Be-7 concentrations can be expected.

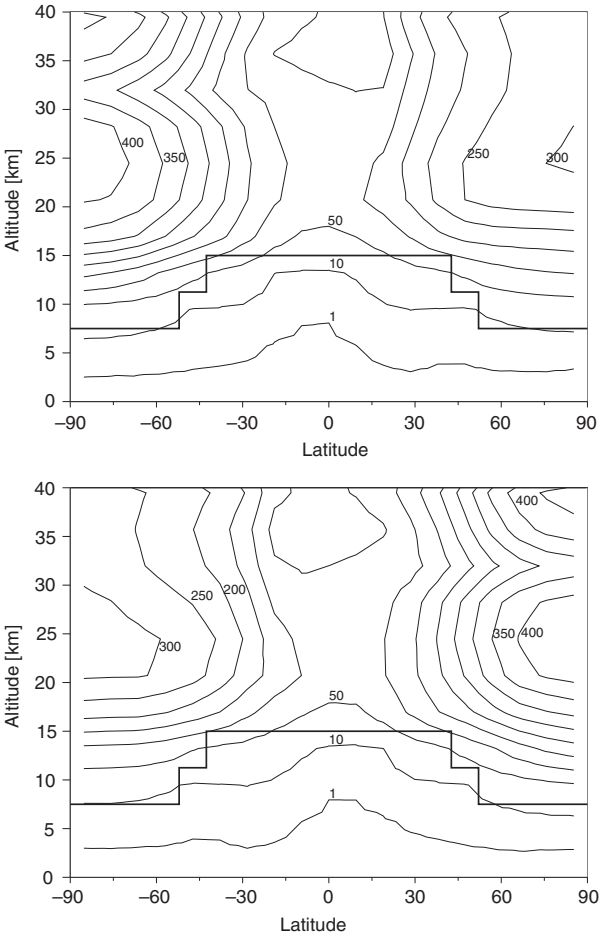

Fig. 6. Simulated concentration of Be-7 in the atmosphere, in 10^4 atoms per standard cubic meter (SCM), for January (top) and July (bottom). The thick line represents the tropopause in the model.

The other difficulty in the model evaluation is that measurements of Be-7 concentrations in the stratosphere are scarce and tend to cover mostly the northern mid and high latitudes. Some measurements, including high up in the stratosphere, were already compiled by Bhandari et al. (1966) and Bhandari (1970), and the largest data set so far has been produced by Jordan et al. (2003), but restricted to the lowest stratosphere. Between 30°N and 70°N and up to 2 km above the tropopause, measurements of stratospheric Be-7 concentrations range from roughly 50 to 250×10^4 atoms/standard cubic meter (SCM), with a maximum close to 350×10^4 atoms/SCM. For such regions, our model predicts concentrations ranging from roughly 50 to 150×10^4 atoms/SCM, which are too low for the high range, even accounting for the solar modulation. For Be-10, measurements

from the same regions indicate values ranging from 80 to 700×10^4 atoms/SCM. For the same regions, our model predicts concentrations ranging from 100 to 200×10^4 atoms/SCM (not shown). High values of 700×10^4 atoms/SCM are simulated only between 20 and 25 km at latitudes higher than 60°N.

It is possible to analyse more finely beryllium observational datasets. Jordan et al. (2003) reported Be-7 measurements made during the SONEX Flight 8, which took place in October 1997 during a period of low solar activity ($\Phi \sim 420$ MV; Usoskin et al., 2011). Aerosols were sampled just above the tropopause at 11–12 km between 61 and 68°N. Be-7 concentrations were found to range from 80 to 270×10^4 atoms/SCM with a mean value of $\sim 220 \times 10^4$ atoms/SCM. Our simulation gives concentrations ranging from 80 to 150×10^4 atoms/SCM, corresponding approximately to the range 100–200×10^4 atoms/SCM when accounting for the low solar activity. For Be-10, measured concentrations are approximately 400×10^4 atoms/SCM, with a range from 130 to 455×10^4 atoms/SCM, whereas simulated values range from 100 to 200×10^4 atoms/SCM. These simulated values are again too low compared to measurements, especially for the range of highest values which are found in our model only at about 15 km. Overall, our simulated concentrations are too low in the tropopause region. This may be due to a poor representation of the vertical gradients prevailing at the tropopause in the 2-D model (not surprising given the coarse spatial resolution of our model), and/or to a poor representation of the polar subsidence.

Concentrations higher in the stratosphere should be less biased in the model because the gradients are certainly much smoother than in the tropopause region. However, few studies have reported beryllium measurements higher up in the stratosphere. Our simulated values of Be-7 concentration match quite well the range of measurements done at 20 km over the ~2 yr period August 1963–April 1965 with low solar activity ($\Phi \sim 400$ to 600 MV; Usoskin et al., 2011), compiled by Bhandari et al. (1966). The simulated values are rather in the upper part of the range, except in sub-tropical latitudes (25–35°N) where they are lower by ~15%. Note that the range of measured values for a given location is quite large, and varies between datasets. For instance, the maximum concentrations reported by Bhandari et al. (1966) range between ~385 (at 20 km) and $\sim 275 \times 10^4$ atoms/SCM (at 15 km), both at 70°N, but higher values have been compiled by Raisbeck et al. (1981) for July 1978 ($\Phi \sim 600$ MV) at 65°N: $\sim 500 \times 10^4$ atoms/SCM between 17 and 19 km, and $\sim 300 \times 10^4$ atoms/SCM at 13.7 km. The corresponding maxima simulated by our model are lower, ~350 (at 20 km) and $\sim 150 \times 10^4$ atoms/SCM (at 14 km).

A similar discrepancy holds for maxima in Be-10 concentration: Raisbeck et al. (1981) reported values of $\sim 1200 \times 10^4$ atoms/SCM for July 1978 at 65°N, whereas our simulated maximum peaks at 700×10^4 atoms/SCM between 20 and 25 km at latitudes higher than 60°N.

Although rather limited in terms of spatial coverage (i.e. northern lower stratosphere), the comparisons between the simulation and measurements suggest that the 2-D model has difficulties reproducing the sharp vertical gradients in the tropopause region and that it possibly underestimates the maximum concentrations in beryllium isotopes. Nonetheless, the model is able to reproduce reasonably well the latitudinal and vertical pattern in beryllium distributions, especially in the higher stratosphere. This provides some confidence in using the model for identifying important processes/mechanisms and diagnosing the budgets and cycles of Be-7 and Be-10 in the stratosphere on large scales. In the following we address two questions: (1) how much particle sedimentation impacts beryllium distribution, and (2) to what extent beryllium isotopes can be used for estimating the aerosol removal rate and the age of air? More specifically, we want to test whether the classical views on the beryllium distribution in the stratosphere is supported by the model; that is, Be-10 distribution is mainly controlled by particle sedimentation, whereas Be-7 distribution is mainly controlled by its radioactive decay (e.g. Lal and Peters, 1967). A better understanding of factors controlling beryllium isotopes distribution, as well as their ratio, should help us to discuss their use as tracers of the mean age of air.

5. Beryllium-10 distribution: impact of sedimentation

Figure 7 shows the annually averaged distribution of Be-10 concentration, expressed in atoms per cubic centimetre (i.e. not converted to STP). Its distribution somehow resembles the distribution of the production rate (Fig. 3), with minima in the tropics and maxima at high latitudes, but with two main differences: (1) Concentrations are very low in the troposphere, at least an order of magnitude lower than stratospheric concentrations, due to the strong scavenging imposed in the model troposphere, and (2) the concentration maxima are found at higher altitudes than the production rate maxima (at about 17 km instead of ~12–15 km). The total atmospheric burden of Be-10 is $\sim 2.8 \times 10^{24}$ atoms, of which 4% are found in the troposphere, 95% in the stratosphere and 1% above, based on the model tropopause definition. These key figures are summarised in Table 1. In the following, we will use the term 'middle atmosphere' to refer to the part of the model above the tropopause, which is essentially the stratosphere.

Since the half-life of Be-10 is longer, by many orders of magnitude, than its atmospheric residence time, its only

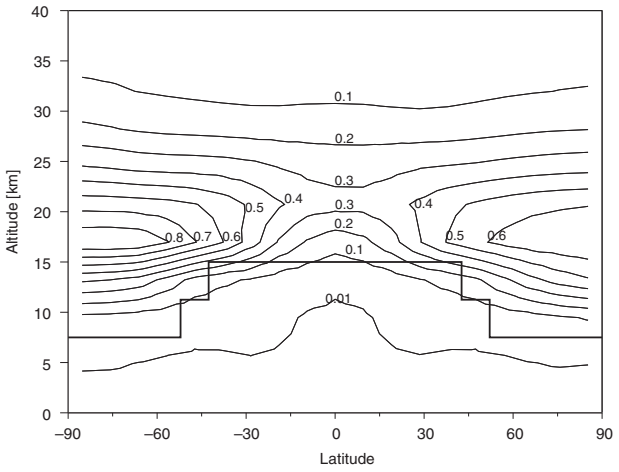

Fig. 7. Simulated annual concentration of Be-10, in atoms per (real) cubic centimetre. The thick line represents the tropopause in the model.

sink is deposition onto the surface of the Earth. As tropospheric Be-10 concentrations are very small compared to stratospheric concentrations, the flux of Be-10 from the troposphere into the stratosphere is negligible compared to the in situ production from GCR. At steady state, the entire middle atmospheric production is balanced by the stratospheric flux of Be-10 into the troposphere where it is removed. The residence time of Be-10 in the middle atmosphere, calculated as the ratio of its burden to its production, is slightly more than 11 months. For the troposphere, there are two sources, the GCR-driven production and the stratospheric flux, and hence the residence time has to be calculated with respect to the total source. The residence time is then about 9 d (compared to 23 d if calculated with respect to only the tropospheric production).

In the stratosphere, sedimenting particles entrain Be-10 atoms downward: the importance of this process in determining Be-10 distribution can be evaluated in the model by preventing the Be-10 atoms to sediment along with aerosol particles. Apart from production, the mechanisms still affecting Be-10 atoms are then transport (by advection and diffusion), and scavenging (by precipitation) in the troposphere. When sedimentation is switched off, the total burden of atmospheric Be-10 is increased by a factor of 2, mainly above the troposphere so that its middle atmosphere residence time is also increased by a factor of 2 (Table 1). Figure 8 shows the change in the Be-10 concentration: it increases above the tropopause, by a factor of $\sim$2 at 20–25 km, and by up to 5 in the tropical high stratosphere (35–40 km). Hence, aerosol sedimentation plays an important role in determining Be-10 concentration and distribution in the model. Especially in the 'tropical pipe', it prevents a substantial part of the beryllium to be advected upward. This suggests that any change in the sedimentation of particles, especially by the massive injection of volcanic sulphur, would have an important effect on the Be-10 distribution in the stratosphere. In the troposphere, Be-10 concentration is less affected by sedimentation because scavenging is so intense. We note that a similar test was conducted by Koch and Rind (1998), with results qualitatively similar. However, they used two different model versions, one with an atmosphere restricted to the first $\sim$30 km, and this somehow prevents quantifying the role of sedimentation.

6. Beryllium-7 distribution: importance of its radioactive decay

Contrary to Be-10, Be-7 decays with a relatively short period ($\sim$77 d) that is comparable to the mean age of air in the lowermost stratosphere (Fig. 1). Measurements show that Be-7 concentrations are indeed lower than their secular equilibrium in the stratosphere, at least up to $\sim$20 km, which indicates that transport (advection/diffusion, sedimentation) contributes significantly to the removal of Be-7 from the lower stratosphere (e.g. Bhandari et al. 1966). On the other hand, other studies (e.g. Lal and Peters, 1967;

Table 1. Key figures about Be-10 and Be-7 determined in this study (note that 'middle atmosphere' stands for the model domain above the tropopause)

	Control simulation		Simulation without sedimentation	
	Be-10	Be-7	Be-10	Be-7
Production rate (atoms/s) and middle atmosphere proportion	1.5×10^{17} 62%	3.3×10^{17} 68%	1.5×10^{17} 62%	3.3×10^{17} 68%
Atmospheric burden (atoms) and middle atmosphere proportion	2.8×10^{24} 96%	1.2×10^{24} 91%	5.5×10^{24} 98%	1.2×10^{24} 92%
Middle atmosphere residence time with respect to production (months)	11.4	1.8	22.7	1.8
Tropospheric residence time (days)	9 wrt. total production	11 wrt. tropospheric production	9 wrt. total production	11 wrt. tropospheric production

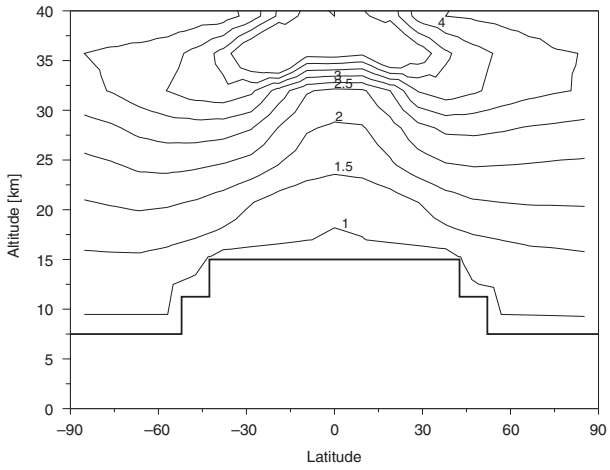

Fig. 8. Ratio of Be-10 concentrations simulated without and with sedimentation of particles.

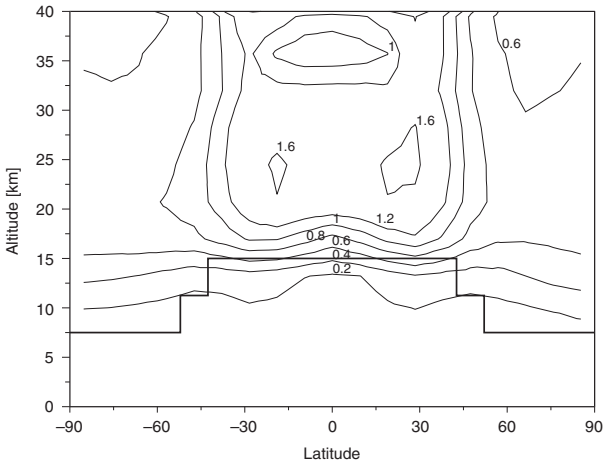

Fig. 9. Ratio of simulated Be-7 concentration to the calculated Be-7 concentration at 'secular equilibrium' (balance between production and radioactive decay), also called 'saturation ratio'.

Land and Feichter, 2003) concluded that most of Be-7 atoms decay in the stratosphere before crossing the tropopause and reaching the surface. Clearly, since most of the Be-7 production takes place at low altitudes (75% below 20 km, cf. Fig. 3 for Be-10, the production pattern for Be-7 is very similar), the fraction of Be-7 atoms that may be removed from the lower stratosphere by transport to the troposphere before decaying by radioactivity could be very significant.

To help disentangling the respective importance of transport vs. production and radioactive decay in determining Be-7 concentration, we calculate how close Be-7 concentration is from its so-called secular equilibrium, that is, the steady-state concentration corresponding to the balance between production and radioactive decay:

$$(\text{Be-7})_{\text{sec}} = P_7/\lambda_7, \quad (1)$$

where P_7 is the Be-7 production rate and λ_7 its radioactive decay rate ($\lambda_7 \sim 1/77\,\text{d}^{-1}$, calculated with a half-life of 53.3 d).

Figure 9 shows the saturation ratio $(\text{Be-7})/(\text{Be-7})_{\text{sec}}$ between the simulated Be-7 concentration and its secular equilibrium. Above $\sim$17–18 km, this ratio is higher than 1 in the tropics (up to 1.6) and close to 0.7 at higher latitudes. Below that level, the ratio is substantially lower than 1.

To interpret the values of this ratio, we follow a phenomenological approach adopted by geochemists since the 1950s for describing various reservoirs. In our case, following Lal and Peters (1967) and Raisbeck et al. (1981), we consider a tropospheric air mass with negligible Be-7 concentration entering the stratosphere at time t_o. The build-up of the Be-7 concentration due to its 'irradiation' by nucleons (the production, P_7) can be written:

$$(\text{Be-7})_t = (\text{Be-7})_{\text{sec}} \times \frac{P_7+Q_7}{P_7} \times \frac{\lambda_7}{\lambda_r+\lambda_7} \times (1 - e^{-(\lambda_r+\lambda_7)(t-t_0)}), \quad (2)$$

where Q_7 and λ_r are, respectively, the input flux and removal rate of Be-7 atoms by advection/diffusion and sedimentation, and $(t - t_o)$ is the time elapsed since the air mass has entered the stratosphere. The first two terms are the relative importance of the production and of the radioactive decay in the total source and sink of Be-7, respectively; the third term describes the build-up of the concentration. If we use the simulated mean age of air (Fig. 1) for the time $(t - t_o)$, this third term increases with altitude and is higher than 0.9 above $\sim$15 km (above $\sim$18 km in the tropics), that is, $\sim$30% higher than the simulated ratio $(\text{Be-7})/(\text{Be-7})_{\text{sec}}$ up to $\sim$18–20 km. These results are not sensitive to the value assumed for λ_r. Hence, the simulated distribution of the $(\text{Be-7})/(\text{Be-7})_{\text{sec}}$ ratio (Fig. 9) can only be explained by a substantial sink (λ_r) of Be-7 in the lower stratosphere in addition to radioactive decay, and by a substantial source (Q_7) of Be-7 in addition to production in the middle and high tropical stratosphere. These additional sink and source are consistent with the effects of the general stratospheric circulation: descending air and sedimentation at mid and high latitudes, and rising air in the tropics both decrease this saturation ratio, and the meridional circulation advects beryllium into the 'tropical pipe'. Such a tropical enrichment was already described in the GISS model by Koch and Rind (1998), with mid- and high-latitude productions contributing to the Be-7 concentration in the tropics above $\sim$15 km ($\sim$25% at 20 km to $\sim$40% at 25 km).

An independent estimate of the importance of radioactive decay in determining the Be-7 concentration is provided by its averaged stratospheric residence time, which is the mean time spent by Be-7 atoms in the stratosphere. If all Be-7 atoms produced in the stratosphere were to decay

before reaching the troposphere, the stratospheric burden as a whole would correspond to its secular equilibrium value, and the residence time of Be-7 in the stratosphere would equal its mean life ($\sim$77 d). Instead, the residence time calculated from our simulation is about 54 d $\sim$1.8 month (Table 1), which means that the inverse of the average removal rate λ_r of Be-7 by transport (advection/diffusion, sedimentation) to the troposphere is $(1/54–1/77)^{-1} \sim$ 6 months. The total stratospheric sink (i.e. export to the troposphere plus radioactive decay) is equal to $(\lambda_r+\lambda_7) \times$ $(\text{Be-7})_{st}$, with $(\text{Be-7})_{st}$ the total stratospheric burden. Hence the export of Be-7 atoms to the troposphere ('stratospheric leak' equal to $\lambda_r \times (\text{Be-7})_{st}$) represents an average fraction $(\lambda_r/(\lambda_r+\lambda_7) = 1\text{-}\lambda_7/(\lambda_r+\lambda_7) \sim 1–54/77)$ of 30% of the total stratospheric sink. This proportion corresponds well with the average value of 0.7 for the simulated ratio $(\text{Be-7})/(\text{Be-7})_{sec}$ in the stratosphere outside the tropics (Fig. 9). This proportion is also expected to be higher at mid-to-high latitudes above the tropopause where exchanges with the troposphere are stronger, as indicated by the low values of the simulated ratio $(\text{Be-7})/(\text{Be-7})_{sec}$ in these regions. Note that to calculate its stratospheric residence time, the input flux of Be-7 atoms from the troposphere has been neglected compared to the total production of Be-7. This input should be very small because the air entering the stratosphere has a far lower concentration in Be-7 than stratospheric air (Fig. 6).

To help us identifying whether it is transport (advection plus diffusion), or sedimentation of Be-7 atoms, which contributes most to enhancing the sink in the stratosphere, we calculate the stratospheric residence time of Be-7 atoms when preventing their sedimentation. The residence time only increases by about 1 d (55 instead of 54 d; a difference not noticeable in Table 1). Hence, contrary to Be-10, sedimentation of Be-7 atoms does not seem to play an important role in removing Be-7 out of the stratosphere, because radioactive decay and transport are faster processes. Nonetheless, sedimentation may still influence the redistribution of Be-7 within the stratosphere.

We note an apparent disagreement between the stratospheric turnover rates (or residence times) of Be-10 and Be-7. For Be-10, it is about 11 months and corresponds to its removal by the transport of air and by sedimentation. For Be-7, correcting the residence time for the radioactive decay leaves us with a residence time of about 6 months, which should also correspond to its removal by the transport of air and by sedimentation. In other words, advection/diffusion and sedimentation do not affect Be-10 and Be-7 on the same timescales. It is not surprising because the effects of these transport processes depend on the actual distributions of Be-10 and Be-7. As a result, the associated timescales can only be comparable if Be-10 and Be-7 were true tracers of air with similar global distributions.

7. Beryllium isotopes as quantitative tracers of stratospheric air

Some studies have used both beryllium isotopes as tracers of stratospheric air injected into the troposphere, based on their elevated stratospheric concentrations and/or elevated ratio (e.g. Dibb et al., 1994; Jordan et al., 2003). Raisbeck et al. (1981) proposed to use the Be-10/Be-7 ratio to calculate the removal rate λ_r of beryllium isotopes from an air mass and infer the residence time of air in the stratosphere. However, this inference is based on two hypotheses. Firstly, that this removal of beryllium isotopes is entirely due to radioactive decay and/or mixing of air masses, and we showed previously that it is not the case for Be-10 in our model. Secondly, that beryllium concentrations are close to steady state, which is not the case in the lowermost stratosphere, as shown by measurements of Be-7 concentrations (see above). They are not close to steady state because of a short age of air and because of seasonal variations, as can be seen on Fig. 6.

Note that we calculate the 'age of air' in the model following Waugh and Hall (2002) approach (see details in Section 2.3). Other metrics (e.g. transit time, Bolin and Rodhe, 1973) and other approaches (e.g. statistical distribution of the age, Waugh and Hall, 2002) do exist to characterise the transport timescale, but exploring them is clearly out of the scope of this study.

Our model allows us to test whether the simulated Be-10/Be-7 ratio is indeed a quantitative indicator of the simulated mean age of air. Since measurements exist for this ratio, we first check that our model gives realistic values of it.

The production rate of Be-10 (P_{10}) is everywhere lower than the one of Be-7 (P_7), with a P_{10}/P_7 ratio ranging from 0.32 to 0.8 (Fig. 5 and Section 3), that is, a P_7/P_{10} ratio ranging roughly from 1.2 to 3. Since radioactive decay adds up to the removal of Be-7, the concentration ratio Be-10/Be-7 is higher than the production ratio P_{10}/P_7. For a tropospheric air mass almost free of beryllium entering the stratosphere, the concentration ratio Be-10/Be-7 increases from the production ratio to a limit determined by sources and sinks [eq. (1) of Raisbeck et al., 1981]. Figure 10 shows the distribution of the concentration ratio simulated by the model for January, one of the periods with the most contrasted conditions. This ratio can be directly compared to the production ratio of Fig. 5. As expected, the concentration ratio shows a general increase with altitude. It is higher than 1 above approximately 10 km, except in the northern tropics where subsidence brings air with ratio higher than 1 down to $\sim$4 km. It is higher than 2 above $\sim$15 km and higher than 5 in the high tropical stratosphere. Below 10 km, the ratio is very close to the production ratio P_{10}/P_7, which means that their concentrations are hardly allowed to build-up and the Be-10/Be-7 ratio to increase.

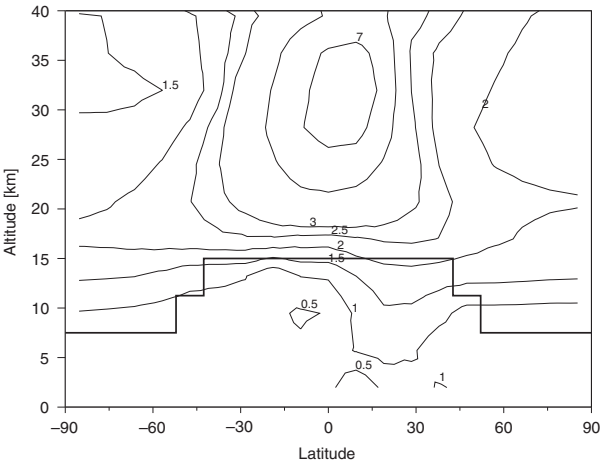

Fig. 10. Ratio of simulated Be-10 to Be-7 concentrations for January.

This simulated distribution of the Be-10/Be-7 concentration ratio is relatively close to the one simulated by Koch and Rind (1998), although the latter values seem higher in general. Plate 1 of Koch and Rind (1998) is difficult to read in details, but it seems that the simulated values of this ratio is higher by 30–50% for January, especially in the lower polar stratosphere, compared to our simulated values. Also, the strong gradient in the lowermost tropical stratosphere seems to be higher in their simulation (above 20 km) than in our simulation ($\sim$15 km, i.e. just above the tropopause).

The largest data set of beryllium measurements has been produced by Jordan et al. (2003). It shows that values of Be-10/Be-7 ratio range generally from 0.5 to 2 through the troposphere and the mid and high lowermost stratosphere up to $\sim$10 km. Between 10 and 12 km, higher values up to $\sim$3.5 are found. Such high values are not simulated in the model below $\sim$16 km and are restricted to the tropical stratosphere. Stratospheric samples from the SONEX Flight 8 (see Section 4), collected between 62 and 68°N and 10–12 km, give values ranging from 1.6 to 2 (with about 15% of uncertainty). Our simulated values corresponding roughly to this flight are somehow lower, between 1 and 1.5. Again, this bias is likely to be due to an insufficient subsidence at high latitudes of air with a high ratio.

Following the method of Lal and Peters (1967) and Raisbeck et al. (1981), we calculate for each grid cell the 'residence time' τ of aerosols of an air mass as:

$$\tau = \frac{1}{\lambda_r} = \frac{1}{\lambda_7} \times \left(\frac{\text{Be-10}}{\text{Be-7}} . \frac{P_7}{P_{10}} - 1 \right). \qquad (3)$$

Note that previous studies used a production ratio close to 0.5 (0.5 in Raisbeck et al., 1981; and 0.6 ± 0.1 in Dibb et al., 1994), whereas we use the simulated, variable one (Fig. 5), which has the effect to increase the residence time by 20–30%. For the whole stratosphere, it is difficult to find any global compact correlation between this residence time and the simulated mean age of air, or any monotonous relationships. Only at high latitudes and for the lower stratosphere does such a monotonous relationship exist, as shown by Fig. 11: residence time and mean age of air do increase with altitude somehow proportionally, with a 1-to-1 ratio between 10 and 13 km and with a 1-to-4 ratio higher up. This means that the residence time τ calculated by eq. (3) underestimates the age of air by several years above $\sim$13 km. Preventing sedimentation of beryllium isotopes improves the general relationship (approx. 1-to-2 ratio; Fig. 11). This shows again that sedimentation adds up to the transport of aerosols by advection/diffusion and reduces their residence time by a factor of $\sim$2.

We have tested other estimates of residence time by applying eq. (2) separately to Be-10 and Be-7 concentrations. However, none of them displays any monotonous relationship with the mean age of air or, if any, none is as close to the 1-to-1 ratio as the one based on the Be-10/Be-7 ratio. Hence, our simulation suggests that a quantitative estimate of the mean 'age of air' based on beryllium isotopes may be restricted to a limited part of the stratosphere, the lowermost stratosphere at mid and high latitudes.

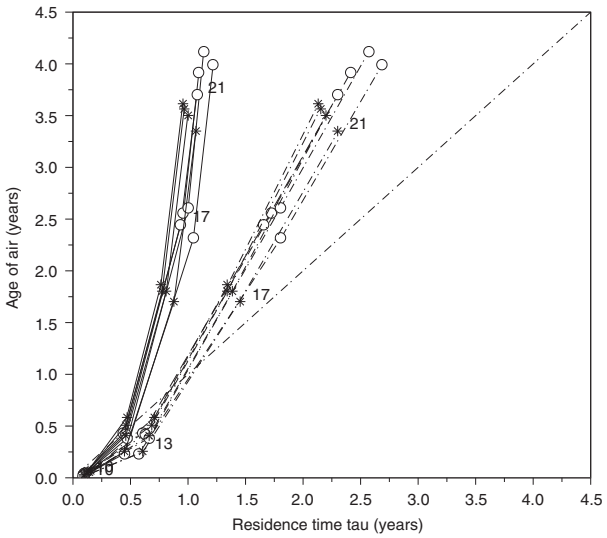

Fig. 11. Simulated vertical profiles of age of air vs. residence time τ of aerosols. Four levels are represented, at approximately 10, 13, 17 and 21 km (cf. labels). Full lines: simulation with beryllium sedimentation; dashed–dotted lines: simulation without sedimentation. Circles underline southern high-latitude profiles (approx. 85°S to 57°S); stars underline northern high-latitude profiles (approx. 85°N to 57°N).

8. Summary and concluding remarks

We present here a modelling study of the global stratospheric cycle and budget of beryllium isotopes, which is probably the first one with such a detailed treatment of the stratospheric processes. This study addresses not only the budget of these isotopes but also the respective importance of transport (with air), sedimentation (with particles), and (for Be-7) radioactive decay, on determining their concentration and distribution in the stratosphere. It is found that transport and sedimentation are about equally important for determining the Be-10 concentration and distribution. Radioactive decay is the main process determining the Be-7 concentration, with transport contributing significantly in the lowermost stratosphere.

The results presented here have implications for the interpretation of beryllium measurements in air and snow. When using these measurements for tracing stratospheric air, as well as for the reconstruction of solar activity, one has to keep in mind that beryllium isotopes concentrations (and ratio, secondarily) depend not only on solar activity but also on stratospheric aerosol loading and on the strength of the stratospheric circulation, with the latter possibly changing because of climate change (WMO, 2011). Note that stratospheric aerosol load is highly variable and can increase by more than two orders of magnitude following large volcanic eruptions. Hence, it is not straightforward to disentangle the different origins of beryllium variability in the surface, as already shown by numerous studies based on surface measurements (e.g. Baroni et al., 2011).

With respect to the use of beryllium isotopes ratio as indicator of the age of stratospheric air, we have shown that the heterogeneity of their production ratio introduces a systematic bias on the estimated age. Further, the model-calculated relationship between the isotopic ratio and the age of air is found monotonic, but not constant, which suggests that the isotopic ratio may only be used as a semi-quantitative indicator of the age of air.

9. Acknowledgements

We are indebted to Ilya Usoskin and Gennady Kovaltsov for taking so much care in estimating the productions of beryllium isotopes and for providing tabulated results. We also thank the reviewers for their constructive comments. We acknowledge fundings from the Agence Nationale de la Recherche projects VolSol (ANR-09-BLAN-0003-01) and VANISH (ANR-07-VULN-013), as well as from the FP7 European project Past4Future. We are also indebted to the Scilab Consortium for the Scilab tool used for calculations and graphs.

References

Baroni, M., Bard, E., Petit, J.-R., Magand, O. and Bourlès, D. 2011. Volcanic and solar activity, and atmospheric circulation influences on cosmogenic ^{10}Be fallout at Vostok and Concordia (Antarctica) over the last 60 years. *Geochim. Cosmochim. Acta.* **75**(22), 7132–7145. DOI: 10.1016/j.gca.2011.09.002.

Bekki, S. 1995. Oxidation of volcanic SO_2: a sink for stratospheric OH and H_2O. *Geophys. Res. Lett.* **22**(8), 913–916. DOI: 10.1029/95GL00534.

Bekki, S. and Pyle, J. A. 1992. Two-dimensional assessment of the impact of aircraft sulphur emissions on the stratospheric sulphate aerosol layer. *J. Geophys. Res.* **97**(D14), 15839–15847.

Bekki, S. and Pyle, J. A. 1994. A two-dimensional modeling study of the volcanic eruption of Mount Pinatubo. *J. Geophys. Res.* **99**(D9), 18861–18869. DOI: 10.1029/94JD00667.

Bhandari, N. 1970. Transport of air in the stratosphere as revealed by radioactive tracers. *J. Geophys. Res.* **75**(15), 2927–2930. DOI: 10.1029/JC075i015p02927.

Bhandari, N., Lal, D. and Rama, D. 1966. Stratospheric circulation studies based on natural and artificial radioactive tracer elements. *Tellus.* **18**(2–3), 391–406. DOI: 10.1111/j.2153-3490.1966.tb00250.x.

Bolin, B. and Rodhe, H. 1973. A note on the concepts of age distribution and transit time in natural reservoirs. *Tellus.* **25**(1), 58–62. DOI: 10.1111/j.2153-3490.1973.tb01594.x.

Brasseur, G. P. and Solomon, S. 2005. *Aeronomy of the Middle Atmosphere. Chemistry and Physics of the Stratosphere and Mesosphere*, Vol. 32, Atmospheric and Oceanographic Sciences Library, Springer, Dordrecht, The Netherlands, 646 pp.

Brost, R. A., Feichter, J. and Heimann, M. 1991. Three-dimensional simulation of ^{7}Be in a global climate model. *J. Geophys. Res.* **96**(D12), 22423–22445. DOI: 10.1029/91JD02283.

Bunzel, F. and Schmidt, H. 2013. The Brewer-Dobson circulation in a changing climate: impact of the model configuration. *J. Atmos. Sci.* **70**(5), 1437–1455. DOI: 10.1175/JAS-D-12-0215.1.

Chipperfield, M. P. and Pyle, J. A. 1988. Two-dimensional modelling of the Antarctic lower stratosphere. *Geophys. Res. Lett.* **15**(8), 875–878. DOI: 10.1029/GL015i008p00875.

Crutzen, P. J. 1976. The possible importance of CSO for the sulfate layer of the stratosphere. *Geophys. Res. Lett.* **3**(2), 73–76. DOI: 10.1029/GL003i002p00073.

Dibb, J. E., Meeker, L. D., Finkel, R. C., Southon, J. R., Caffee, M. W. and co-authors. 1994. Estimation of stratospheric input to the Arctic troposphere: ^{7}Be and ^{10}Be in aerosols at Alert, Canada. *J. Geophys. Res.* **99**(D6), 12855–12864. DOI: 10.1029/94JD00742.

Field, C. V., Schmidt, G. A., Koch, D. and Salyk, C. 2006. Modeling production and climate-related impacts on ^{10}Be concentration in ice cores. *J. Geophys. Res.* **111**, D15107. DOI: 10.1029/2005JD006410.

Gleeson, L. J. and Axford, W. I. 1968. Solar modulation of galactic cosmic rays. *Astrophys. J.* **154**, 1011–1026.

Haenel, F. J., Stiller, G. P., von Clarmann, T., Funke, B., Eckert, E. and co-authors. 2015. Reassessment of MIPAS age of air trends and variability. *Atmos. Chem. Phys. Discuss.* **15**(10), 14685–14732. DOI: 10.5194/acpd-15-14685-2015.

Hall, T. M., Waugh, D. W., Boering, K. A. and Plumb, R. A. 1999. Evaluation of transport in stratospheric models. *J. Geophys. Res.* **104**(D15), 18815–18839. DOI: 10.1029/1999JD900226.

Harwood, R. S. and Pyle, J. A. 1980. The dynamical behaviour of a two-dimensional model of the stratosphere. *Q. J. Roy. Meteorol. Soc.* **106**(449), 395–420. DOI: 10.1002/qj.49710644903.

Heikkilä, U., Beer, J. and Feichter, J. 2008b. Modeling cosmogenic radionuclides ^{10}Be and ^{7}Be during the Maunder Minimum using the ECHAM5-HAM General Circulation Model. *Atmos. Chem. Phys.* **8**(10), 2797–2809. DOI: 10.5194/acp-8-2797-2008.

Heikkilä, U., Beer, J. and Feichter, J. 2009. Meridional transport and deposition of atmospheric ^{10}Be. *Atmos. Chem. Phys.* **9**, 515–527. DOI: 10.5194/acp-9-515-2009.

Heikkilä, U., Beer, J., Jouzel, J., Feichter, J. and Kubik, P. 2008a. ^{10}Be measured in a GRIP snow pit and modeled using the ECHAM5-HAM general circulation model. *Geophys. Res. Lett.* **35**, L05817. DOI: 10.1029/2007GL033067.

Jordan, C. E., Dibb, J. E. and Finkel, R. C. 2003. ^{10}Be/^{7}Be tracer of atmospheric transport and stratosphere-troposphere exchange. *J. Geophys. Res.* **108**(D8), 4234. DOI: 10.1029/2002JD002395.

Junge, C. E. 1963. *Air Chemistry and Radioactivity*. Academic Press, New York, 382 pp.

Koch, D. and Rind, D. 1998. Beryllium 10/beryllium 7 as a tracer of stratospheric transport. *J. Geophys. Res.* **103**(D4), 3907–3917. DOI: 10.1029/97JD03117.

Koch, D., Schmidt, G. A. and Field, C. V. 2006. Sulfur, sea salt and radionuclide aerosols in GISS ModelE. *J. Geophys. Res.* **111**, D06206. DOI: 10.1029/2004JD005550.

Koch, D. M., Jacob, D. J. and Graustein, W. C. 1996. Vertical transport of tropospheric aerosols as indicated by ^{7}Be and ^{210}Pb in a chemical tracer model. *J. Geophys. Res.* **101**(D13), 18651–18666. DOI: 10.1029/96JD01176.

Kodera, K. and Kuroda, Y. 2002. Dynamical response to the solar cycle. *J. Geophys. Res.* **107**(D24), 4749. DOI: 10.1029/2002JD002224.

Kovaltsov, G. A. and Usoskin, I. G. 2010. A new 3D numerical model of cosmogenic nuclide ^{10}Be production in the atmosphere. *Earth Planet. Sci. Lett.* **291**(1–4), 182–188. DOI: 10.1016/j.epsl.2010.01.011.

Lal, D. and Peters, B. 1962. Cosmic ray produced isotopes and their application to problems in geophysics. In: *Progress in Elementary Particle and Cosmic Ray Physics* (eds. J. G. Wilson and S. A. Wouthuysen) Vol. 6, North-Holland, Amsterdam, pp. 3–72.

Lal, D. and Peters, B. 1967. Cosmic ray produced radioactivity on the Earth. In: *Encyclopedia of Physics: Cosmic Rays II* (eds. S. Flügge and K. Sitte) Vol. 46. Springer-Verlag, Berlin, pp. 551–612.

Land, C. and Feichter, J. 2003. Stratosphere-troposphere exchange in a changing climate simulated with the general circulation model MAECHAM4. *J. Geophys. Res.* **108**(D12), 8523. DOI: 10.1029/2002JD002543.

Law, K. S. and Pyle, J. A. 1993. Modeling trace gas budgets in the troposphere 1. Ozone and odd nitrogen. *J. Geophys. Res.* **98**(D10), 18377–18400. DOI: 10.1029/93JD01479.

Lifton, N., Smart, D. F. and Shea, M. A. 2008. Scaling time-integrated in situ cosmogenic nuclide production rates using a continuous geomagnetic model. *Earth Planet. Sci. Lett.* **268**(1–2), 190–201. DOI: 10.1016/j.epsl.2008.01.021.

Logan, J. A., Prather, M. J., Wofsy, S. C. and McElroy, M. B. 1981. Tropospheric chemistry: a global perspective. *J. Geophys. Res.* **86**(C8), 7210–7254. DOI: 10.1029/JC086iC08p07210.

Masarik, J. and Beer, J. 1999. Simulation of particle fluxes and cosmogenic nuclide production in the Earth's atmosphere. *J. Geophys. Res.* **104**(D10), 12099–12111. DOI: 10.1029/1998JD200091.

Masarik, J. and Beer, J. 2009. An updated simulation of particle fluxes and cosmogenic nuclide production in the Earth's atmosphere. *J. Geophys. Res.* **114**, D11103. DOI: 10.1029/2008JD010557.

McHargue, L. R. and Damon, P. E. 1991. The global beryllium-10 cycle. *Rev. Geophys.* **29**(2), 141–158. DOI: 10.1029/91RG00072.

Raisbeck, G. M., Yiou, F., Fruneau, M., Loiseaux, J. M., Lieuvin, M. and co-authors. 1981. Cosmogenic ^{10}Be/^{7}Be as a probe of atmospheric transport processes. *Geophys. Res. Lett.* **8**(9), 1015–1018. DOI: 10.1029/GL008i009p01015.

Rehfeld, S. and Heimann, M. 1995. Three dimensional atmospheric transport simulation of the radioactive tracers ^{210}Pb, ^{7}Be, ^{10}Be, and ^{90}Sr. *J. Geophys. Res.* **100**(D12), 26141–26161. DOI: 10.1029/95JD01003.

Sander, S. P., Abbatt, J. R., Barker, J. B., Burkholder, R. R., Friedl, D. M. and co-authors. 2011. *Chemical Kinetics and Photochemical Data for Use in Atmospheric Studies*, Evaluation #17, JPL Publication 10–6, Jet Propulsion Laboratory, California Institute of Technology, Pasadena, CA, 699 pp.

Seinfeld, J. H. and Pandis, S. N. 2006. *Atmospheric Chemistry and Physics: From Air Pollution to Climate Change*. Wiley, Hoboken, New Jersey, 1232 pp.

Sheng, J.-X., Weisenstein, D. K., Luo, B.-P., Rozanov, E., Stenke, A. and co-authors. 2015. Global atmospheric sulfur budget under volcanically quiescent conditions: aerosol-chemistry-climate model predictions and validation. *J. Geophys. Res. Atmos.* **120**(1), 256–276. DOI: 10.1002/2014JD021985.

Smart, D. F. and Shea, M. A. 2003. Geomagnetic cutoff rigidity calculations at 50-year intervals between 1600 and 2000. In: *28th International Cosmic Ray Conference*, Trukuba, Japan, International Union of Pure and Applied Physics (IUPAP), pp. 4201–4204.

SPARC. 2006. Assessment of stratospheric aerosol properties (ASAP). In: *Stratospheric Processes and Their Role in Climate (SPARC)* (eds. L. Thomason and T. Peter), SPARC report 4, 348 pp. Online at: http://www.sparc-climate.org/publications

Stier, P., Feichter, J., Kinne, S., Kloster, S., Vignati, E. and co-authors. 2005. The aerosol-climate model ECHAM5-HAM. *Atmos. Chem. Phys.* **5**(4), 1125–1156. DOI: 10.5194/acp-5-1125-2005.

Stohl, A., Bonasoni, P., Cristofanelli, P., Collins, W., Feichter, J. and co-authors. 2003. Stratosphere-troposphere exchange: a review, and what we have learned from STACCATO. *J. Geophys. Res.* **108**(D12), 8516. DOI: 10.1029/2002JD002490.

Turco, R. P., Whitten, R. C. and Toon, O. B. 1982. Stratospheric aerosols: observation and theory. *Rev. Geophys.* **20**(2), 233–279. DOI: 10.1029/RG020i002p00233.

Usoskin, I. G., Bazilevskaya, G. A. and Kovaltsov, G. A. 2011. Solar modulation parameter for cosmic rays since 1936

reconstructed from ground-based neutron monitors and ionization chambers. *J. Geophys. Res.* **116**(A2), A02104. DOI: 10.1029/2010JA016105.

Usoskin, I. G., Field, C. V., Schmidt, G. A., Leppänen, A.-P., Aldahan, A. and co-authors. 2009. Short-term production and synoptic influences on atmospheric ^{7}Be concentrations. *J. Geophys. Res.* **114**, D06108. DOI: 10.1029/2008JD011333.

Usoskin, I. G. and Kovaltsov, G. A. 2008. Production of cosmogenic ^{7}Be isotope in the atmosphere: full 3-D modeling. *J. Geophys. Res.* **113**, D12107. DOI: 10.1029/2007JD009725.

Waugh, D. and Hall, T. 2002. Age of stratospheric air: theory, observations, and models. *Rev. Geophys.* **40**(4), 1010. DOI: 10.1029/2000RG000101.

World Meteorological Organization (WMO). 2011. *Scientific Assessment of Ozone Depletion: 2010*, WMO, Global Ozone Research and Monitoring Project report 52, Geneva, 516 pp. Online at: https://www.wmo.int/pages/prog/arep/gaw/ozone/index.html

World Meteorological Organization (WMO). 2014. *Scientific Assessment of Ozone Depletion: 2014*, WMO, Global Ozone Research and Monitoring Project report 55, Geneva, 416 pp. Online at: https://www.wmo.int/pages/prog/arep/gaw/ozone/index.html